Role of endometrial stromal and epithelial primary cells in matrix-free spheroid assembly: Insight into the early initiation of endometriosis

POLLYANA T. NOGUEIRA, MARAIR G.F. SARTORI, EDUARDO SCHOR, ALEXANDER KOPELMAN and ADRIANA L. INVITTI

Department of Gynecology, Paulista School of Medicine, Federal University of Sao Paulo, Sao Paulo, SP 04024-002, Brazil

Received February 10, 2024; Accepted July 16, 2024

DOI: 10.3892/wasj.2024.271

Abstract. The etiopathology of endometriosis is poorly understood, and retrograde menstruation continues to be the most accepted theory to explain its development. Endometrial stromal cells (eSCs) and endometrial epithelial cells (eECs) have been extensively studied to elucidate their role in the establishment of disease. The present study evaluated the role of eSCs and eECs in the formation of endometrial spheroids in a matrix-free model resembling regurgitated endometrial cells in the peritoneal environment. Primary eSCs and eECs were isolated from the eutopic endometrium of women with stage IV endometriosis (n=4) and cocultured at different cell type ratios (eSCs:eECs: group HS, 9:1; group SE, 1:1; and group HE, 1:9). The morphology of the spheroids and the participation of each cell type were evaluated by microscopy. The eSCs were the main part of the spheroids at all ratios assessed and were in the inner part of the spheres. The increase in the proportion of eSCs was directly proportional to the increase in spheroid size. On day 3, the HS group had a radius of 37 μm (SD ±9.90), the SE group had a radius of 24 μm (SD ±4.17) and the HE group had a radius of 20 μm (SD ±5.40). The spheroids were mainly composed of an eSCs core surrounded by an eECs lining. The mesenchymal stem cell marker, CD146, was expressed even by the cells on the surface of the spheroids, which should be epithelial. On the whole, the present study demonstrates that, both eECs and eSCs actively contribute to the formation of endometrial spheroids. Interactions between eSCs and eECs are required for the formation of stable spheroids, underscoring the putative role of eECs and eSCs crosstalk in cell survival in peritoneal fluid.

Correspondence to: Miss Pollyana T. Nogueira, Department of Gynecology, Paulista School of Medicine, Federal University of Sao Paulo, 608 Napoleão de Barros Road, Vila Clementino, Sao Paulo, SP 04024-002, Brazil
E-mail: pollyanatelles@gmail.com

Key words: endometriosis, endometrial cells, stromal cells, epithelial cells, spheroids

Introduction

Endometriosis is a chronic gynecological disease that affects ~10% of females of reproductive age (1). It is characterized by the presence of endometrium-like tissue outside the uterine cavity, mainly in the peritoneal cavity, ovaries, bladder and intestine (2). Endometriotic implants respond to sex steroids, in the same manner as the endometrium, characterizing endometriosis as a hormone-dependent condition (3).

Since the first description of endometriosis, its etiopathogenesis has been extensively studied. However, despite extensive efforts made in this direction over the past decade, none of the theories described can explain all presentations of the disease. The most commonly accepted theory is the theory of retrograde menstruation (the implantation or Sampson theory), which states that endometriosis is the result of the implantation and establishment of viable endometrial cells regurgitated through the fallopian tubes (4). However, retrograde menstruation occurs in ~80% of females of reproductive age with pervious tubes (5).

Thus, further research is required to elucidate the putative role of retrograde menstruation in the pathophysiology of endometriosis. Retrograde menstruation, a type of menstrual effluent, involves growth factors, cytokines, and immune and endometrial cells that can be packed in cell condensates (6,7), but not endometrial tissue fragments (8). Clonal mesenchymal stem cells can also be found in menstrual effluent (6,9), and their role in endometriosis has been discussed since their first identification (10).

In order to elucidate the mechanisms and to propose therapeutic approaches for endometriosis, numerous *in vitro* and *in vivo* models of the disease have been proposed (2,11,12). Rodent models are the main *in vivo* models but they are limited by the species-specific differences (rodents do not develop endometriosis spontaneously) (2,13,14), and the tissue explant mice models are limited by the availability of female tissues and the duration of the cultures by residual immune response from the host (11,15). In addition, the results obtained from these models may be related to the method of endometriosis induction, and the association between inflammation and disease cannot be adequately addressed (2). The non-human primate models are very close to the physiology

and immunology observed in females; however, they raise several ethical concerns and are a very costly (11,16-19). Due to all these reasons, the *in vitro* models became a suitable and effective alternative for the study of endometriosis.

The most applied *in vitro* model is the monolayer (bi-dimensional) culture of primary, lineages or immortalized cells (2,11,12). It provides crucial data on the specific cell types and cell-to-cell interactions (12); however, it cannot mimic the complete peritoneal and/or endometrial environment (11,12,14,18), lacking the essential feedback that occurs in *in vivo* tissue (14). The translation of this model into clinical practice is very limited (2).

Being closer to *in vivo* physiology than the majority of other models, the three-dimensional ones are promising, and highly novel, for the study of endometriosis pathophysiology, mirroring cell phenotypes and gene expression, and allowing the study of different cell interactions and mechanisms (18). The three-dimensional models are able to mimic the human tissues features as cellular organization and interaction to extracellular matrix and between cells (20). The matrix dependent three-dimensional cultures are the most commonly applied three-dimensional model for the study of endometriosis (21-23). The first two models developed employed only endometrial epithelial cells (eECs) (22,23) and most recently, a model also including endometrial stromal cells (eSCs) was developed (24). Those models are able to resemble the eutopic endometrium physiology (22-24) and mimic the interactions between cells and extracellular matrix, but not the behaviour of endometrial cells in the matrix-free environment, such as peritoneal fluid (25,26).

According to this, the matrix-free model is the better choice of model for studying the endometrial cells regurgitated through the fallopian tubes (26), as the peritoneal cavity is a fluid environment constantly moving within abdominopelvic compartments (27,28). eSCs and eECs are able to form spheroids in matrix-free three-dimensional models resembling cell condensates found in menstrual effluent (14,29). Menstrual effluent presents different ratios between epithelial and stromal cells, with eSCs being abundantly viable than eECs (30,31). Patients with endometriosis appear to have an increased number of stromal cells in their menstrual effluent (31,32).

It is well known that interactions between co-cultured epithelial and stromal cells can activate epithelial cells and lead to cell polarization and phenotypic changes (33). The majority of the cells shed in menstrual effluent are senescent (32) and are not viable for long periods of time without an attachment surface. However, a lack of extracellular matrix has been linked to the switch in endometrial cells from undergoing apoptosis to undergoing epithelial-to-mesenchymal transition (EMT) (34), which is a phenotypic cell change characterized by changes in cell-to-cell contact, cytoskeleton architecture, cell polarity and motility (35). This switch can be related to the survival of cells in the peritoneal cavity and the early initiation of endometriosis (36).

The present study aimed to characterize the spheroids formed by the two main endometrial cell types, stromal and epithelial primary cells, and to elucidate the mechanisms involved in the formation of stable cellular structures in a peritoneal fluid-like environment. A better understanding of these mechanisms may contribute to the elucidation of the mechanisms involved in the early initiation of endometriosis.

Materials and methods

Human tissues and cell culture. The study protocol was approved by the Universidade Federal de São Paulo Ethics Committee (study no. 1054/2021 part of the main project no. 0875/2018, São Paulo, Brazil), and informed written consent was obtained from all patients. Human endometrial samples were collected from four cycling women (n=4) (details of the patients are presented in Table SI) undergoing laparoscopic surgery or at an outpatient clinic at the Pelvic Pain and Endometriosis Unit of the Federal University of São Paulo, São Paulo, Brazil. The samples were collected between August, 2020 and March, 2022. Endometrium biopsies were collected using a pipelle curette (Laboratoire CCD) from four (n=4) cycling women aged 18-40 years who were examined at the gynecology outpatient clinic and met the following inclusion criteria: They had revised American Society of Reproductive Medicine (rASRM) stage IV endometriosis, had not taken exogenous hormones and had not given birth or breastfed over the past 3 months prior to sample collection. Patients who presented with comorbidities, such as adenomyosis, uterine fibroids, teratomas, myoma or other endometrial and pelvic inflammatory diseases were not included in the study.

Cells were isolated from endometrial biopsies from a modified protocol based on previously described protocols (33,37). The endometrial tissue was washed twice with phosphate-buffered saline pH 7.4 (PBS; MilliporeSigma) and minced into smaller sections. The tissue fragments were digested in Dulbecco's modified Eagle's medium with nutrient mixture F12 (DMEM:F12) (Thermo Fisher Scientific, Inc.) containing 255 units of collagenase type IA (MilliporeSigma) and incubated for 30 min in a 37˚C water bath under constant agitation. Following the digestion, the cell and fragments suspension was filtrated with a 40-μm cell strainer to separate single eSCs and endometrium epithelial sheets and glands. eSCs, single cells that have passed through the strainer, were inoculated in eSC medium: DMEM:F12 pH 7.4, 1% Minimum Essential Medium non-essential amino acids (Gibco; Thermo Fisher Scientific, Inc.), 0.1 mmol/l 2-mercaptoethanol (MilliporeSigma), 100 U/ml penicillin and 100 μg/ml streptomycin and 10% fetal bovine serum (FBS; Gibco; Thermo Fisher Scientific, Inc.) into a 25 cm^2 cell culture flask. The epithelial clusters retained in the 40-μm strainer were inoculated in EC medium: DMEM-F12, pH 7.4, 100 U/ml penicillin and 100 μg/ml streptomycin, 2.5 mM FBS, 2.5 mM Nu-Serum (Corning, Inc.) and 1% of L-glutamine into a pre-coated collagen type IV (MilliporeSigma) 35 mm dish. The isolated cells were characterized as stromal and epithelial through the detection of vimentin [1:100 Vimentin (Alexa 488), cat. no. 562338] and cytokeratin [1:50 Pan-cytokeratin-phycoerythrin (PE); cat. no. 347204; BD Biosciences] expression by fluorescence microscopy (Fig. S1). The detailed staining method is described below.

Living cell co-culture spheroid assay. Calcein (green or orange) was reconstituted to 1 mg/ml in DMSO (MilliporeSigma) according to the manufacturer's

protocol. The eSCs were labeled with 10 μM calcein-AM (cat. no. C3100MP, Invitrogen; Thermo Fisher Scientific, Inc.) diluted in eSC medium and the eECs with 10 μM RedOrange-Calcein-AM (cat. no. C34851, Invitrogen; Thermo Fisher Scientific, Inc.) diluted in eEC medium and incubated for 15 min at 37˚C/5% CO_2, prior to cell dissociation for co-culture assay. Cells were dissociated from the culture flasks and suspended in SP medium (DMEM:F12 pH 7.4, 1% Minimum Essential Medium non-essential amino acids (Gibco; Thermo Fisher Scientific, Inc.), 0.1 mmol/l 2-mercaptoethanol (MilliporeSigma), 100 U/ml penicillin and 100 μg/ml streptomycin and 2 mM L-glutamine). The cell concentration and viability were determined using a Countess™ Cell Counter (Thermo Fisher Scientific, Inc.) with the cells were stained with trypan blue 0.4% (Thermo Fisher Scientific, Inc.) 1:2 sample dilution factor at room temperature for 30 sec. The two cell types were mixed at three different ratios of eSCs:eECs as follows: 9:1 for the highly stromal (HS) group, 1:1 for the equal ratio (SE) group and 1:9 for the highly epithelial (HE) group. The mixed cell suspensions were seeded at a density of 10,000 cells per well into 24-well ultralow attachment plates (CELLSTAR™, Cell-Repellent Surface; Greiner Bio-One). Living spheroids were visualized by fluorescence microscopy on an EVOS™ FL Digital Inverted Microscope (AMG-Advanced Microscopy Group) using the channels GFP (470 nm excitation, 525 nm emission) and RFP (531 nm excitation, 593 nm emission) at 1, 2 and 3 days after seeding.

Spheroid assay. Non-stained eSCs and eECs were dissociated from culture flasks and suspended in SP medium. The two cell types were mixed at three different eSC:eEC ratios: 9:1 for the HS group (highly stromal), 1:1 for the SE group (equal ration) and 1:9 for the HE group (highly epithelial). The mixed cell suspensions were seeded at a density of 10,000 cells per well into 24-well ultralow attachment plates (CELLSTAR®, Cell-Repellent Surface; Greiner Bio-One). Fresh media SP medium was added every 3-4 days. Spheroids were visualized using brightfield microscopy with an AxioVert PrimoVert microscope, and images were taken with Zen 2012 (blue edition) software (Carl Zeiss Microscopy GmbH 2011). Images were recorded at 3, 7 and 15 days after seeding. The morphological characteristics of the spheroids were assessed using ImageJ (FIJI) Macro INSIDIA 2.0, software version 2.9.0; Java 1.8.0_322 (64-bit).

Viability assay. The viability of the spheroids was assessed after 15 days of culture. The spheroids were labelled with 10 μM calcein-AM (cat. no. C3100MP, Invitrogen; Thermo Fisher Scientific, Inc.) and 1 μg/ml Hoescht 33342 (Sigma-Aldrich, Merck KGaA) added to each well and incubated at 37˚C 5% CO_2 for 15 min. Medium was partially removed (70% of total medium in the well) and the same volume of fresh medium added. Spheroids were visualized in EVOS™ FL Digital Inverted Microscope (AMG-Advanced Microscopy Group) using the channels GFP (470 nm excitation, 525 nm emission) for calcein detection (cytoplasm) and DAPI (357 nm excitation, 447 nm emission) for Hoescht 33342 detection (nuclei).

Immunofluorescence assay. Spheroids were labeled using direct immunofluorescence method which applies primary fluorophore-conjugated antibodies without a secondary antibody step. Spheroids were fixed with 4% paraformaldehyde (PFA) (MilliporeSigma) for 15 min and permeabilized with 0.3% Triton X-100 solution in phosphate buffer (pH 7.4; PBS) for 10 min, at room temperature. Unspecific sites were blocked with 2% bovine serum albumin (BSA) solution in PBS for 30 min at room temperature. Spheroids were stained for 1 h at room temperature in PBS pH 7.4 with 0.2% BSA buffer containing one of the conjugated antibodies pairs: Vimentin [1:100 Vimentin (Alexa 488); cat. no. 562338] and pancytokeratin [1:50 Pan-Cytokeratin (PE); cat. no. 347204; BD Biosciences] or the cell surface glycoprotein MUC18 [1:50 CD146-Fluorescein isothiocyanate (FITC); cat. no. 560846; BD Biosciences] and integrin-β1 [1:200 CD29 (PE); cat. no. 556049; BD Biosciences]. The control slides were prepared in the same manner and stained with the fluorophore pairs used in the testing slides. The isotype controls used were the following: Immunoglobulin G1 (IgG1) isotype controls conjugated with PE (cat. no. 550617, BD Biosciences), FITC (cat. no. 555909, BD Biosciences) and Alexa 488 (cat. no. 557702, BD Biosciences) at the same concentrations as the conjugated antibodies. The nuclei were stained with 4',6-diamidino-2-phenylindol (DAPI) (MilliporeSigma) in PBS pH 7.4 for 15 min at room temperature. Spheroid images were captured using an EVOS™ FL Digital Inverted Microscope (AMG-Advanced Microscopy Group) with the following channels: DAPI (357 nm excitation, 447 nm emission), GFP (470 nm excitation, 525 nm emission) and RFP (531 nm excitation, 593 nm emission).

Statistical analysis. All cell cultures and experiments were performed in triplicate. Numeric variables are presented as the mean and standard deviation. Measurements were compared using the Kruskal-Wallis test, and pairwise comparisons were performed using the Mann-Whitney U test. Comparisons over time were calculated using repeated-measures and mixed effects ANOVA. The reported P-values for the pairwise comparisons were adjusted by the Dunn-Bonferroni adjustment. The data were analyzed using IBM SPSS Statistics version 2. A P-value <0.05 was considered to indicate a statistically significant difference (95% confidence).

Results

Role of eSCs and eECs in spheroid assembly and structure. The spheroids had different morphologies and structural organizations depending on the ratio of eSCs to eECs. The proportions of eSCs and eECs in the cell aggregates formed on day 1 were determined for the HS and HE groups (Fig. 1A and G). The seeding of equal amounts of eSCs and eECs (group SE) resulted in a greater proportion of stromal cells forming cell aggregates on day 1 (Fig. 1D). Furthermore, none of the seeds had a spheroid-like structure on day 1.

The HS group had a spheroid structure at 2 days after seeding; eECs were found at the surface of the spheroid, and eSCs occupied the center (Fig. 1B). Compared with those in the HS group, the spheroids in the SE and HE groups were smaller (Fig. 1E and H). The distribution of eECs and eSCs

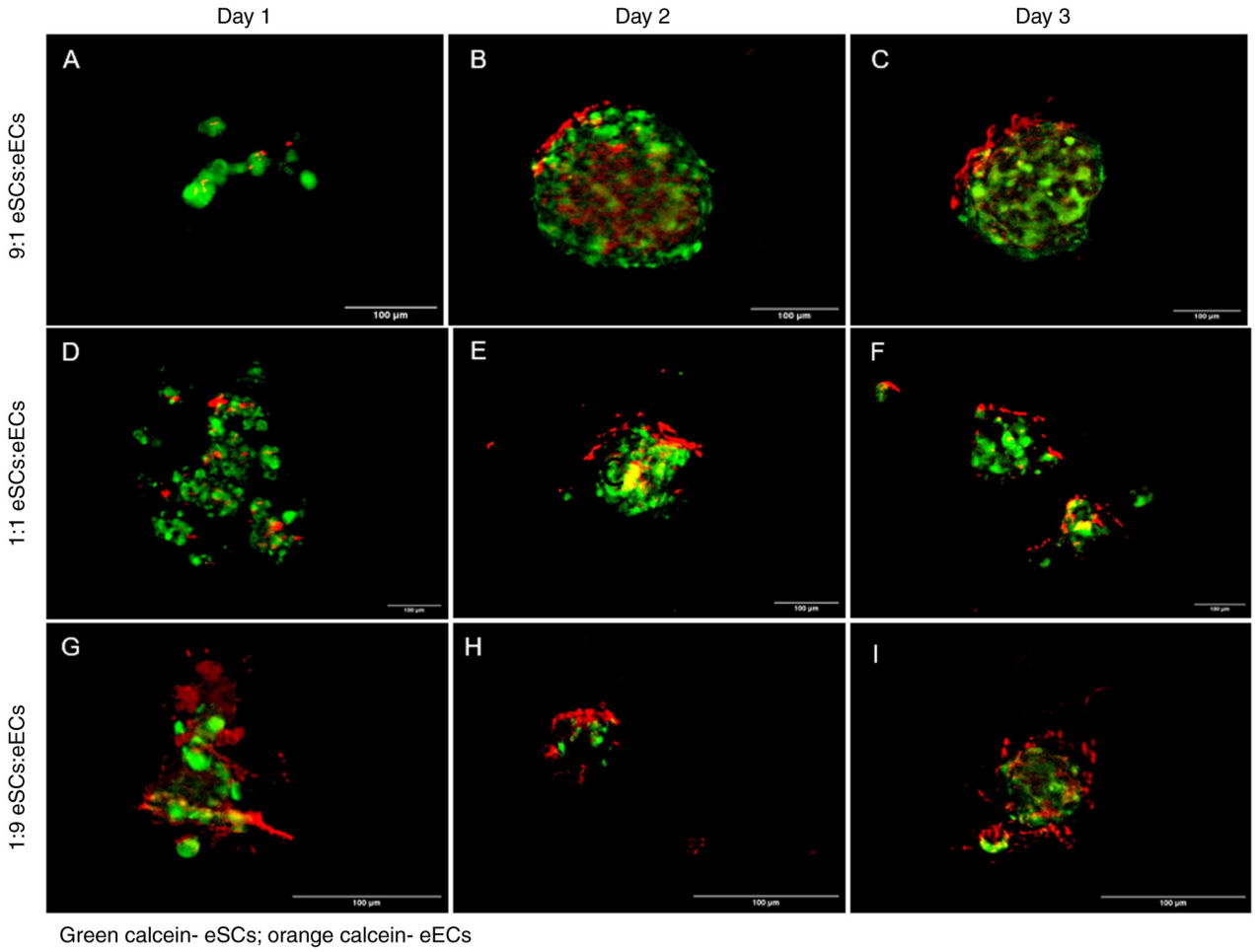

Figure 1. Images of cell aggregates and spheroids with different eSC and eEC seeding ratios. The eSCs were labeled with calcein-AM (green), and the eECs are labeled with RedOrange-Calcein-AM (red). (A-C) Fluorescence microscopy for the HS group (9:1 eSC:eEC ratio; highly stromal) on days 1, 2 and 3, respectively; (D-F) fluorescence microscopy for the SE group (1:1 eSC:eEC ratio; equal ratios) on days 1, 2 and 3, respectively; (G-I) fluorescence microscopy for the HE group (1:9 eSC:eEC ratio; highly epithelial) on days 1, 2 and 3, respectively. All images were obtained at the same magnification (x10) and laser powers. Scale bars, 100 μm. eSCs, endometrial stromal cells; eECs, endometrial epithelial cells.

was the same as that in the HS group. Groups SE and HE formed spheroids with less circularity.

The fluorescent signal of calcein was still faint at 3 days after seeding. The size, structure, cellularity and circularity remained the same for the HS group (Fig. 1C). The spheroids formed in the SE group had a non-spherical structure on day 3 (Fig. 1F). The spheroids in the HE group maintained their general structure and circularity, but the inner part appeared to be filled with eSCs (Fig. 1I).

Spheroid assembly and evolution over time. Spheroids with different eEC and eSC contents were imaged (Fig. 2A-I) and measured at 3, 7 and 15 days after seeding. The main measurement used for analysis was the radiusE, which was calculated using the optimal fit ellipse to a single spheroid. At 3 days after seeding, the HS group formed one spheroid per well with a radius ranging from 30 to 50 μm (mean, 37 μm; SD ±9.90), while the SE group formed 12 spheroids with radii ranging from 18 to 28 μm (mean, 24 μm; SD ±4.17), and the HE group formed 10 spheroids with radii ranging from 13 to 28 μm (mean, 20 μm; SD ±5.40). Spheroids from the HS group were significantly larger than those from the HE group (P=0.008; Fig. 2J).

On day 7, the HS group had spheroids ranging from 30 to 48 μm (mean, 38 μm; SD ±6.71), the SE group had spheroids ranging from 25 to 38 μm (mean, 30 μm; SD ±4.80) and the HE group had spheroids ranging from 20 to 31 μm (mean, 25 μm; SD ±4.67) (P=0.011; Fig. 2K). The spheroids did not change in radius significantly between days 3 and 7, for all groups (HS, P=0.999; SE, P=0.640; and HE, P=0.999). The spheroids from the SE and HE groups became smaller after 15 days of co-culture (comparison to day 7, P<0.001 and P=0.015, respectively). Measurements at 15 days followed the patterns observed at 3 and 7 days of co-culture. The HS group had larger spheroids (radiusE mean, 31 μm; SD ±4.10) than the SE group (mean, 14 μm; SD ±3.55) and the HE group (mean, 15 μm; SD ±6.80) (P=0.009) (Fig. 2L). The spheroids from the SE group became smaller after 15 days of co-culture (comparison to HE, P=0.999 and HS, P=0.001 and to SE on day 7, P<0.001). Over time, the spheroids in the HS group were more stable and larger than the spheroids in the SE and HE groups (P<0.001; Fig. 2M). Spheroids remained viable after 15 days of co-culture (Fig. S2).

Immunocytofluorescence characterization of the cells composing the spheroids. The eECs and eSCs were

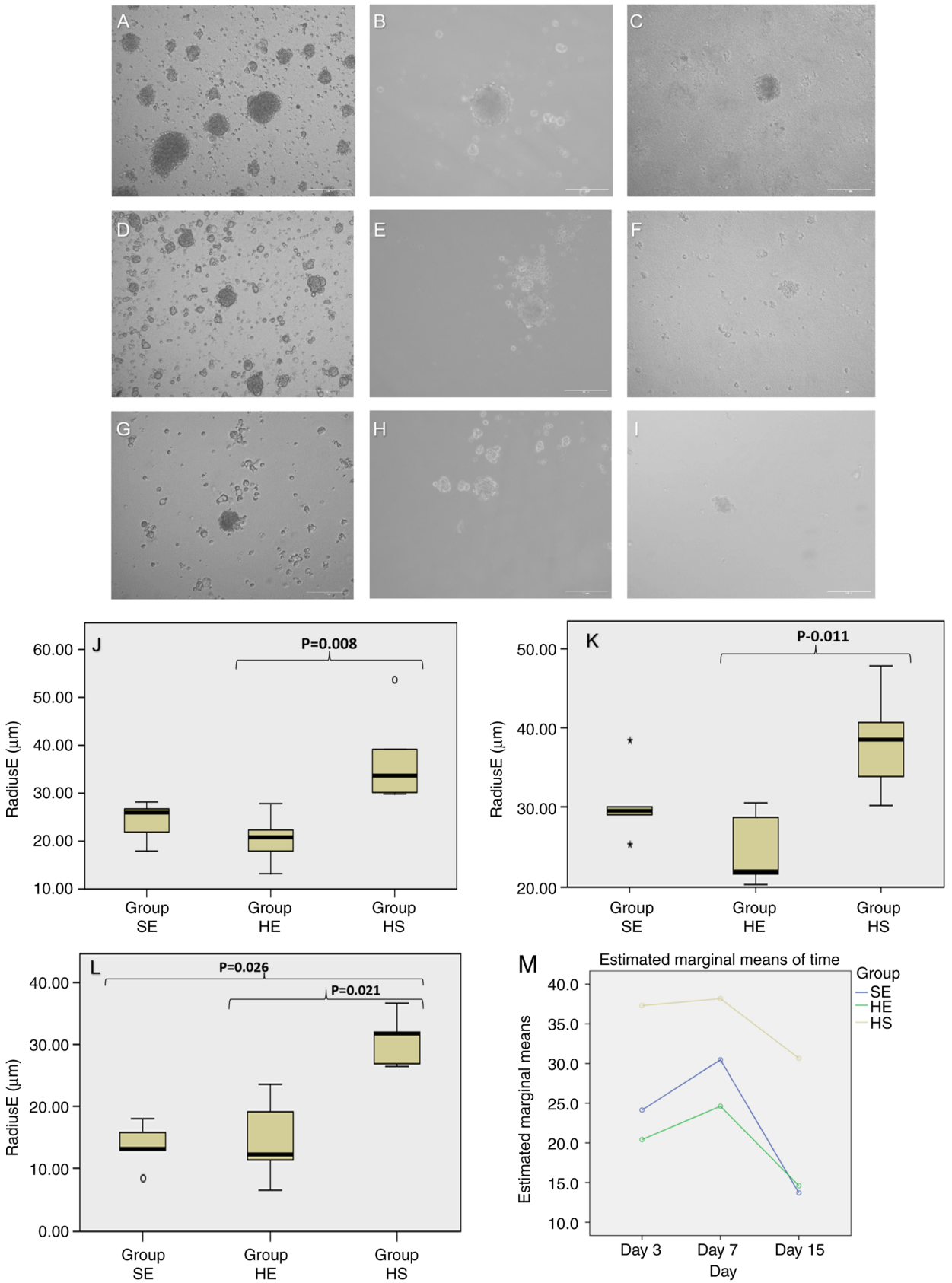

Figure 2. Brightfield microscopy images of the spheroids at 3, 7 and 15 days after seeding. (A-C) Images from the HS group (9:1 eSC:eEC ratio; highly stromal); (D-F) images from the SE group (1:1 eSC:eEC ratio; equal ratios); (G-I) images from the HE group (1:9 eSC:eEC ratio; highly epithelial). Scale bars, 100 μm. (J) Boxplot representing the RadiusE (μm) from spheroids on day 3. (K) Boxplot representing the RadiusE (μm) from spheroids on day 7. (L) Boxplot representing the RadiusE (μm) from spheroids on day 15; y axis, Radius E in μm; x axis, experimental groups [HS (9:1 eSCs:eECs), SE (1:1 eSCs:eECs) and HE (1:9 eSCs:eECs)]. (M) Changes in spheroid radius E over time; x axis, time in days (3, 7 and 15 days after seeding); y axis, marginal estimated means for radiusE calculated using repeated measures ANOVA and mixed effects ANOVA; green curve, HE group (1:9 eSC:eEC ratio; highly epithelial); blue curve, SE group (1:1 eSC:eEC ratio; equal ratio); yellow curve, HS group (9:1eSC:eEC ratio; highly stromal). Mauchly's W=0.729, P=0.176; within subjects by day (P<0.001) and the day and group (P=0.598) and between subjects (type) (P<0.001). eSCs, endometrial stromal cells; eECs, endometrial epithelial cells.

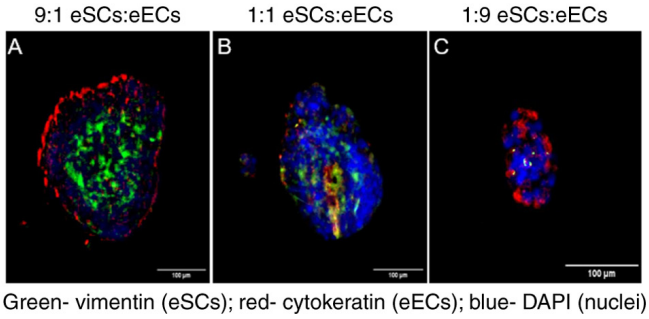

Figure 3. Fluorescence microscopy images of spheroids assembled with different ratios of eECs and eSCs on day 7. Images show vimentin in green (Alexa488), cytokeratin in red (PE) and nuclei in blue (DAPI). (A) HS group (9:1 eSCs:eECs ratio; highly stromal), (B) SE group (1:1 eSC:eEC ratio; equal ratios), (C) HE group (1:9 eSC:eEC ratio; highly epithelial). All images were obtained at the same magnification (x10) and laser powers. Scale bars, 100 μm). eSCs, endometrial stromal cells; eECs, endometrial epithelial cells.

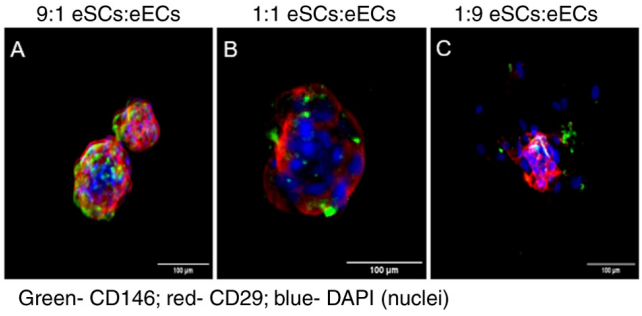

Figure 4. CD146-FITC (green) and CD29-PE (red) staining of spheroids on day 7. Nuclei were stained with DAPI (blue). (A) HS group (9:1 eSCs:eECs ratio; highly stromal), (B) SE group (1:1 eSCs:eECs ratio; equal ratios) and (C) HE group (1:9 eSCs:eECs ratio; highly epithelial). Scale bars, 100 μm. eSCs, endometrial stromal cells; eECs, endometrial epithelial cells.

characterized as epithelial and stromal by the expression of vimentin and cytokeratin, respectively (Fig. S1). Images of the cells stained with calcein demonstrated that the spheroids were composed of both epithelial and stromal cells. The phenotype of the cells in the spheroids was confirmed by the presence of vimentin, cytokeratin, CD29 and CD146 in the spheroids on day 7 after seeding. Vimentin and cytokeratin staining corroborated the calcein living cell results, as cytokeratin markers were detected in the cells on the surface of the spheroids, and vimentin was detected in the inner part of the spheroids (Fig. 3), reinforcing the polarity of the epithelial cells and their tendency toward the lining.

Notably, the amount of CD146 staining was high even in the HE group, which was expected to have the smallest quantity of mesenchymal cells as seeds with a smaller amount of eSCs. The greater the concentration of eSCs, the greater the expression of CD146. The cells on the surface of the spheroids expressed not only cytokeratin (Fig. 3), but also the mesenchymal markers, CD29 and CD146 (Fig. 4), mainly in the HS and SE groups. These results indicated that these cells may have changed their phenotype during cell aggregation. The HE group exhibited a CD29 signal only at the inner part of the spheroid, with no CD146 signal in the cells at the surface (Fig. 4C).

Discussion

The present study developed a three-dimensional *in vitro* model to mimic the Sampson theory for the early initiation of endometriosis by means of co-culturing endometrial epithelial and stromal primary cells in a matrix-free culture system. According to Sampson, endometrial cells are regurgitated through the fallopian tubes and remain viable in the peritoneal environment (4). The peritoneal cavity is a liquid environment and peritoneal fluid is constantly moving within the abdominopelvic cavity (27,28). The areas where peritoneal fluid stagnation occurs correspond to the main areas where endometriotic implants are located, which corroborates the Sampson theory (28). Retrograde menstruation occurs in almost every cycle of the endometrium (38); thus, peritoneal disease can be fed in each cycle and its early initiation can be related to the first menstrual cycles.

Nevertheless, the Sampson theory does not explain how endometrial cells remain viable until they reach the stagnation points or a surface to attach. The present study observed that eECs were able to form stable structures, spheroids, in a matrix-free (liquid) environment. Stejskalová *et al* (39) reported the ability of eSCs only to form spheroids in hanging-drop assays and described their ability to form endometriosis lesion-like structures in collagen and Matrigel matrixes. The spheroids are able to attach to surfaces, indicating the putative mechanism of the formation of endometriosis peritoneal implants. The present study included eECs in the stromal cell model, as menstrual effluent contains all the main cells shed from the eutopic endometrium, stromal and epithelial cells (30,31).

The present study observed that the structure, morphology and viability of spheroids formed by primary endometrial cells without a supporting matrix was dependent on the proportions of cocultured eSCs and eECs. The greater the proportion of stromal cells, the greater the spheroid radius and circularity. The radius of spheroids seeded with equal amounts of stromal and epithelial cells decreased with time, as the spheroids seeded with larger amounts of epithelial cells (1:9 eSCs:eECs) were larger in size on day 7 compared with day 3, although the size then diminished. The radius of all spheroids diminished over time. These changes in radius may be due to cell death or spheroid compaction, and an increase in spheroid size may be related to cell proliferation or an increase in the inner cavity. As the present study did not measure cell proliferation and/or death, the mechanisms behind the changes in spheroid radius cannot be explained. These findings indicate a key role for eSCs in cell survival in the peritoneal environment. Considering that the menstrual effluent from women with endometriosis have larger amounts of stromal cells (31,32), these results reinforce the key role of stromal cells in the pelvic endometriosis pathogenesis.

Three-dimensional models of eECs supported by a matrix display a gland-like structure, with an empty cavity forming the organoids (23,40). Only stromal cell spheroids have a compact structure without a cavity (39). Epithelial cells are characterized by distinct organelles, membrane domains, and lipid and protein apical and basal polarity that are necessary for their proper function (41). Cell polarity is not only observed in epithelial cells, but is also crucial for stem cell fate and

division (42). Cell polarity could be clearly observed in the co-cultures described in the present study work, with stromal cells located in the inner part of the spheroids and epithelial cells located on the surface forming a lining. Co-cultures of epithelial and stromal cells usually display this distribution, as epithelial cells are confined to the outer layer due to their polarity, and stromal cells function as a support for epithelial cells and remain within the sphere (43,44), similar to the structure observed *in vivo* (29). This cell type distribution reflects a dynamic interaction between the cells and indicates that cell-to-cell interactions are relevant for survival in a matrix-free environment (29,44).

This polarity of the epithelial cells to the surface of the spheroid (43) was expected; of note however, these cells expressed mesenchymal cell markers (CD146 and CD29). This can indicate a putative transition to an intermediary stromal phenotype, as the cells were marked with different living cell markers, and the epithelial phenotype was detected only on the surface of the spheroids. These intermediary phenotypes have been described in the endometriosis endometrium and implants, with the promotion of EMT in endometriotic tissues (45,46). EMT is suggested to be one of the key mechanisms for endometriosis initiation and lesion development (47).

Recently, a model using endometrial cell lines grown as spheroids achieved similar results for epithelial cell polarity, but without revealing phenotypic changes (44). Song *et al* (44), observed the same distribution of epithelial (surface) and stromal cells (inner part) in the spheroid structure, but did not report changes in the phenotypic markers as done in the present study. The present study examined whether the cells retained the epithelial and stromal markers and observed that even the cells in the surface of the spheroid expressed stromal/mesenchymal markers. This observation may be due to the use of primary cells instead of cell lines. Cell lines, due to immortalization process, display different metabolic profiles from primary cells (41,48). Some organ-specific characteristics and tissue-related phenotypes are lost in the immortalization process and the cells also carry epigenetic changes (48-50). The cell physiology mechanisms most affected in the cell lines are those related to mitochondrial activity, changes in the epigenetic patterns and the promotion of cell cycle mechanisms (48,49). Considering that endometriosis cells have been described to have several cell cycle impairments (51), caution should be used with the use of cell lines without primary cells for comparisons (48,49,52).

The presence of CD146-positive cells in spheroids indicates the presence of endometrial mesenchymal stem cells (eMSCs), which are related to the pathogenesis of endometriosis (53). eMSCs are abundant in menstrual effluent (6,9), and their ability to survive in peritoneal fluid through spheroids can corroborate the retrograde menstruation theory (10,54). Recently, different cell phenotypes were identified in the menstrual effluent of endometriosis patients; the majority of these cells are immune cells, although there are also changes in the mesenchymal cell content (32). Endometriosis also exhibit differences in the expression of genes related to TGF-β pathways and the EMT mechanism SNAIL-1 (55). The *in vitro* physiology results presented in the present study relate these previous findings to the ability of eutopic endometriosis cells to survive in a matrix-free environment. However, further studies on immune cells, peritoneal fluid and the diversity of cells contained in the menstrual effluent, as well as the attachment process and secreted factors that can be related to the implant establishment (e.g., VEGF, IL-8, IL-1β and TGF-β) are warranted to confirm the results presented herein. The authors are currently carrying out some of these *in vitro* studies, evaluating the EMT mechanisms involved in the spheroids formation and attachment including also mesothelial cells and peritoneal fluid. In addition, the spheroid model is being applied to test the effect of drugs in the formation of spheroids, that can indicate putative benefits for pelvic endometriosis treatment. Additionally, the authors have standardized the sample to include only peritoneal deep infiltrating disease; thus, the results can provide insight into the early initiation of peritoneal implants, but not other endometriosis presentations, such as endometriomas.

In conclusion, eSCs play essential roles in the formation of endometrial spheroids. Spheroid assembly may be the mechanism through which menstrual effluent cells survive in the peritoneal fluid and avoid immune cell clearance. This model may aid the elucidation of the mechanisms responsible for the early initiation of endometriosis.

Acknowledgements

Not applicable.

Funding

The present study was supported by Fundação de Amparo à Pesquisa do Estado de São Paulo (FAPESP, Brazil; grant no. 2018/11508-9) and Conselho Nacional de Desenvolvimento Científico e Tecnológico (National Counsel of Technological and Scientific Development, CNPQ; grant no. 133590/2020-8).

Availability of data and materials

The datasets used and/or analyzed during the current study are available from the corresponding author on reasonable request.

Authors' contributions

PTN carried out the experiments and was responsible for the acquisition of data. ALI, ES and MGFS were involved in the conception and design of the study. ES and AK were involved in the collection of samples. PTN, ALI, ES, AK and MGFS were involved in the analysis and interpretation of the data. PTN and ALI confirm the authenticity of all the raw data. All authors were involved in the drafting and critical discussion of the manuscript and all authors have read and approved the final version of the manuscript to be published.

Ethics approval and consent to participate

The study protocol was approved by the Universidade Federal de São Paulo ethical committee (Project no. 1054/2021/CAAE no. 51541220.8.0000.5505 part of the main project no. 0875/2018/CAAE no. 94562518.4.0000.5505), and informed written consent was obtained from all patients.

Patient consent for publication

Not applicable.

Competing interests

The authors declare that they have no competing interests.

References

1. Baranov V, Malysheva O and Yarmolinskaya M: Pathogenomics of endometriosis development. Int J Mol Sci 19: 1852, 2018.
2. Zondervan KT, Becker CM, Koga K, Missmer SA, Taylor RN and Viganò P: Endometriosis. Nat Rev Dis Primer 4: 9, 2018.
3. Berkley KJ, Rapkin AJ and Papka RE: The pains of endometriosis. Science 308: 1587-1589, 2005.
4. Sampson JA: Peritoneal endometriosis due to the menstrual dissemination of endometrial tissue into the peritoneal cavity. Am J Obstet Gynecol 14: 422-469, 1927.
5. Liu DT and Hitchcock A: Endometriosis: Its association with retrograde menstruation, dysmenorrhoea and tubal pathology. Br J Obstet Gynaecol 93: 859-862, 1986.
6. Patel AN, Park E, Kuzman M, Benetti F, Silva FJ and Allickson JG: Multipotent menstrual blood stromal stem cells: Isolation, characterization, and differentiation. Cell Transplant 17: 303-311, 2008.
7. van der Linden PJ: Theories on the pathogenesis of endometriosis. Hum Reprod 11 (Suppl 3): S53-S65, 1996.
8. van der Linden PJ, Dunselman GA, de Goeij AF, van der Linden EP, Evers JL and Ramaekers FC: Epithelial cells in peritoneal fluid-of endometrial origin? Am J Obstet Gynecol 173: 566-570, 1995.
9. Rodrigues MCO, Lippert T, Nguyen H, Kaelber S, Sanberg PR and Borlongan CV: Menstrual blood-derived stem cells: In vitro and in vivo characterization of functional effects. In: Biobanking and Cryopreservation of Stem Cells. Advances in Experimental Medicine and Biology. Karimi-Busheri F and Weinfeld M (eds). Vol 951. Springer International Publishing, Cham, pp111-121, 2016.
10. Gargett CE, Schwab KE and Deane JA: Endometrial stem/progenitor cells: The first 10 years. Hum Reprod Update 22: 137-163, 2016.
11. Grümmer R: Models of endometriosis: in vitro and in vivo models. In: Endometriosis: Science and Practice. Giudice LC, Evers JLH and Healy DL (eds). Wiley-Blackwell, Oxford, pp263-269, 2012.
12. Griffith JS, Rodgers AK and Schenken RS: In vitro models to study the pathogenesis of endometriosis. Reprod Sci 17: 5-12, 2010.
13. Davies J: Potential advantages of using biomimetic alternatives. In: Replacing Animal Models. Davies J (ed). Wiley, pp1-11, 2012.
14. Al-Juboori AAA, Ghosh A, Jamaluddin MFB, Kumar M, Sahoo SS, Syed SM, Nahar P and Tanwar PS: Proteomic analysis of stromal and epithelial cell communications in human endometrial cancer using a unique 3D co-culture model. Proteomics 19: e1800448, 2019.
15. Bruner-Tran KL, McConaha ME and Osteen KG: odels of endometriosis: Animal models I-rodent-based chimeric mode. In: Endometriosis: Science and Practice. Giudice LC, Evers JLH and Healy DL (eds). Wiley-Blackwell, Chichester, pp270-284, 2012.
16. King CM, Barbara C, Prentice A, Brenton JD and Charnock-Jones DS: Models of endometriosis and their utility in studying progression to ovarian clear cell carcinoma. J Pathol 238: 185-196, 2016.
17. Braundmeier AG and Fazleabas AT: The non-human primate model of endometriosis: Research and implications for fecundity. Mol Hum Reprod 15: 577-586, 2009.
18. Greaves E, Critchley HOD, Horne AW and Saunders PTK: Relevant human tissue resources and laboratory models for use in endometriosis research. Acta Obstet Gynecol Scand 96: 644-658, 2017.
19. Fazleabas AT: Models of Endometriosis: Animal models II-non-human primates. In: Endometriosis: Science and Practice. 1st edition. Giudice LC, Evers JLH and Healy DL (eds). Wiley Blackwell, Chichester, pp285-291, 2012.
20. Costa EC, de Melo-Diogo D, Moreira AF, Carvalho MP and Correia IJ: Spheroids formation on non-adhesive surfaces by liquid overlay technique: Considerations and practical approaches. Biotechnol J 13: 1700417, 2018.
21. Deane JA, Cousins FL and Gargett CE: Endometrial organoids: In vitro models for endometrial research and personalized medicine. Biol Reprod 97: 781-783, 2017.
22. Boretto M, Cox B, Noben M, Hendriks N, Fassbender A, Roose H, Amant F, Timmerman D, Tomassetti C, Vanhie A, *et al*: Development of organoids from mouse and human endometrium showing endometrial epithelium physiology and long-term expandability. Development 144: 1775-1786, 2017.
23. Turco MY, Gardner L, Hughes J, Cindrova-Davies T, Gomez MJ, Farrell L, Hollinshead M, Marsh SGE, Brosens JJ, Critchley HO, *et al*: Long-term, hormone-responsive organoid cultures of human endometrium in a chemically defined medium. Nat Cell Biol 19: 568-577, 2017.
24. Gnecco JS, Brown A, Buttrey K, Ives C, Goods BA, Baugh L, Hernandez-Gordillo V, Loring M, Isaacson KB and Griffith LG: Organoid co-culture model of the human endometrium in a fully synthetic extracellular matrix enables the study of epithelial-stromal crosstalk. Med 4: 554-579.e9, 2023.
25. Malvezzi H, Marengo EB, Podgaec S and Piccinato CA: Endometriosis: Current challenges in modeling a multifactorial disease of unknown etiology. J Transl Med 18: 311, 2020.
26. Murphy AR, Campo H and Kim JJ: Strategies for modelling endometrial diseases. Nat Rev Endocrinol 18: 727-743, 2022.
27. Pannu HK and Oliphant M: The subperitoneal space and peritoneal cavity: Basic concepts. Abdom Imaging 40: 2710-2722, 2015.
28. Bricou A, Batt RE and Chapron C: Peritoneal fluid flow influences anatomical distribution of endometriotic lesions: Why Sampson seems to be right. Eur J Obstet Gynecol Reprod Biol 138: 127-134, 2008.
29. Wiwatpanit T, Murphy AR, Lu Z, Urbanek M, Burdette JE, Woodruff TK and Kim JJ: Scaffold-free endometrial organoids respond to excess androgens associated with polycystic ovarian syndrome. J Clin Endocrinol Metab 105: 769-780, 2020.
30. Koks CA, Dunselman GA, de Goeij AF, Arends JW and Evers JL: Evaluation of a menstrual cup to collect shed endometrium for in vitro studies. Fertil Steril 68: 560-564, 1997.
31. Warren LA, Shih A, Renteira SM, Seckin T, Blau B, Simpfendorfer K, Lee A, Metz CN and Gregersen PK: Analysis of menstrual effluent: Diagnostic potential for endometriosis. Mol Med 24: 1, 2018.
32. Shih AJ, Adelson RP, Vashistha H, Khalili H, Nayyar A, Puran R, Herrera R, Chatterjee PK, Lee AT, Truskinovsky AM, *et al*: Single-cell analysis of menstrual endometrial tissues defines phenotypes associated with endometriosis. BMC Med 20: 315, 2022.
33. Chen JC, Erikson DW, Piltonen TT, Meyer MR, Barragan F, McIntire RH, Tamaresis JS, Vo KC, Giudice LC and Irwin JC: Coculturing human endometrial epithelial cells and stromal fibroblasts alters cell-specific gene expression and cytokine production. Fertil Steril 100: 1132-1143, 2013.
34. Ruiz-Mitjana A, Navaridas R, Vidal-Sabanés M, Perramon-Güell A, Yeramian A, Felip I, Eritja N, Egea J, Encinas M, Matias-Guiu X and Dolcet X: Lack of extracellular matrix switches TGF-β induced apoptosis of endometrial cells to epithelial to mesenchymal transition. Sci Rep 12: 14821, 2022.
35. Thiery JP, Acloque H, Huang RY and Nieto MA: Epithelial-mesenchymal transitions in development and disease. Cell 139: 871-890, 2009.
36. Kirkwood PM, Gibson DA, Shaw I, Dobie R, Kelepouri O, Henderson NC and Saunders PTK: Single-cell RNA sequencing and lineage tracing confirm mesenchyme to epithelial transformation (MET) contributes to repair of the endometrium at menstruation. Elife 11: e77663, 2022.
37. Luckow Invitti A, Schor E, Martins Parreira R, Kopelman A, Kamergorodsky G, Gonçalves GA and Batista Castello Girão MJ: Inflammatory cytokine profile of co-cultivated primary cells from the endometrium of women with and without endometriosis. Mol Med Rep 18: 1287-1296, 2018.
38. Halme J, Hammond MG, Hulka JF, Raj SG and Talbert LM: Retrograde menstruation in healthy women and in patients with endometriosis. Obstet Gynecol 64: 151-154, 1984.
39. Stejskalová A, Fincke V, Nowak M, Schmidt Y, Borrmann K, von Wahlde MK, Schäfer SD, Kiesel L, Greve B and Götte M: Collagen I triggers directional migration, invasion and matrix remodeling of stroma cells in a 3D spheroid model of endometriosis. Sci Rep 11: 4115, 2021.

40. Boretto M, Maenhoudt N, Luo X, Hennes A, Boeckx B, Bui B, Heremans R, Perneel L, Kobayashi H, Van Zundert I, *et al*: Patient-derived organoids from endometrial disease capture clinical heterogeneity and are amenable to drug screening. Nat Cell Biol 21: 1041-1051, 2019.
41. Inman JL and Bissell MJ: Apical polarity in three-dimensional culture systems: Where to now? J Biol 9: 2, 2010.
42. Florian MC and Geiger H: Concise review: Polarity in stem cells, disease, and aging. Stem Cells 28: 1623-1629, 2010.
43. Kosheleva NV, Efremov YM, Shavkuta BS, Zurina IM, Zhang D, Zhang Y, Minaev NV, Gorkun AA, Wei S, Shpichka AI, *et al*: Cell spheroid fusion: Beyond liquid drops model. Sci Rep 10: 12614, 2020.
44. Song Y, Burns GW, Joshi NR, Arora R, Kim JJ and Fazleabas AT: Spheroids as a model for endometriotic lesions. JCI Insight 8: e160815, 2023.
45. Konrad L, Dietze R, Riaz MA, Scheiner-Bobis G, Behnke J, Horné F, Hoerscher A, Reising C and Meinhold-Heerlein I: Epithelial-mesenchymal transition in endometriosis-when does it happen? J Clin Med 9: 1915, 2020.
46. Chen M, Zhou Y, Xu H, Hill C, Ewing RM, He D, Zhang X and Wang Y: Bioinformatic analysis reveals the importance of epithelial-mesenchymal transition in the development of endometriosis. Sci Rep 10: 8442, 2020.
47. Matsuzaki S and Darcha C: Epithelial to mesenchymal transition-like and mesenchymal to epithelial transition-like processes might be involved in the pathogenesis of pelvic endometriosis. Hum Reprod 27: 712-721, 2012.
48. Pan C, Kumar C, Bohl S, Klingmueller U and Mann M: Comparative proteomic phenotyping of cell lines and primary cells to assess preservation of cell type-specific functions. Mol Cell Proteomics 8: 443-450, 2009.
49. Maqsood MI, Matin MM, Bahrami AR and Ghasroldasht MM: Immortality of cell lines: Challenges and advantages of establishment. Cell Biol Int 37: 1038-1045, 2013.
50. Kaur G and Dufour JM: Cell lines: Valuable tools or useless artifacts. Spermatogenesis 2: 1-5, 2012.
51. Zondervan KT, Becker CM and Missmer SA: Endometriosis. N Engl J Med 382: 1244-1256, 2020.
52. Fan H: In-vitro models of human endometriosis. Exp Ther Med 19: 1617-1625, 2020.
53. Cousins FL, O DF and Gargett CE: Endometrial stem/progenitor cells and their role in the pathogenesis of endometriosis. Best Pract Res Clin Obstet Gynaecol 50: 27-38, 2018.
54. Nayyar A, Saleem MI, Yilmaz M, DeFranco M, Klein G, Elmaliki KM, Kowalsky E, Chatterjee PK, Xue X, Viswanathan R, *et al*: Menstrual effluent provides a novel diagnostic window on the pathogenesis of endometriosis. Front Reprod Health 2: 3, 2020.
55. Penariol LBC, Thomé CH, Tozetti PA, Paier CRK, Buono FO, Peronni KC, Orellana MD, Covas DT, Moraes MEA, Silva WA Jr, *et al*: What do the transcriptome and proteome of menstrual blood-derived mesenchymal stem cells tell us about endometriosis? Int J Mol Sci 23: 11515, 2022.

Copyright © 2024 Nogueira et al. This work is licensed under a Creative Commons Attribution 4.0 International (CC BY 4.0) License.